ELSEVIER

Journal of Alloys and Compounds 317–318 (2001) 44–51

Journal of ALLOYS AND COMPOUNDS

www.elsevier.com/locate/jallcom

^{57}Fe Mössbauer spectroscopy study of the AFe_xAl_{12-x} intermetallics (A=Y, Tm, Lu and U, $4 \leq x \leq 4.3$)

J.C. Waerenborgh[a,*], P. Salamakha[a], O. Sologub[a], A.P. Gonçalves[a], S. Sério[b], M. Godinho[b], M. Almeida[a]

[a]*Departamento de Química, Instituto Tecnológico e Nuclear, P-2686-953 Sacavém, Portugal*
[b]*Departamento de Física, Faculdade de Ciências da Universidade de Lisboa, P-1749-016 Lisboa, Portugal*

Abstract

AFe_xAl_{12-x} intermetallics (A=Y, Tm, Lu and U, $4 \leq x \leq 4.3$) were synthesized as polycrystalline material and as large single crystals by the Czochralski method from bulk charges containing A, Fe and Al in the atomic ratios 1/4/8. The purity of the studied samples was checked by powder X-ray diffraction and their final composition was estimated using the Rietveld method of structure refinement. The ^{57}Fe Mössbauer spectra of samples with final composition $x>4$ have revealed that the Fe atoms on the same crystallographic site may have different magnetic moments, μ_{Fe}, whose values increase with the number of Fe nearest neighbours. The strong sensitivity of the μ_{Fe} on small deviations from the ideal 1/4/8 stoichiometry has clearly shown that while the single crystals of UFe_4Al_8 grown by the Czochralski method have the expected composition, those grown from YFe_4Al_8 and $LuFe_4Al_8$ bulk charges have actual compositions $YFe_{4.2(1)}Al_{7.8(1)}$ and $LuFe_{4.2(1)}Al_{7.8(1)}$ thus explaining contradictory results that have been previously published.

Keywords: Rare-earth iron aluminides; Uranium iron aluminides; Mössbauer spectroscopy; Magnetic properties

1. Introduction

The intermetallic systems AFe_xAl_{12-x} (A=Y or an *f* element and $x \geq 4$), crystallizing in the $ThMn_{12}$-type structure, continue to attract much interest. Compounds such as $DyFe_{11.5}Ta_{0.5}$, $SmFe_{10}Si_2$ or $UFe_{10}Si_2$, with uniaxial anisotropies and high Curie temperatures, $T_{ord} \approx 550$–650 K, suggest that these materials might be potential candidates for permanent magnets with the lowest *f*-element content [1,2]. The *f* element sublattice provides the required anisotropy while the high T_{ord} is due to the strong Fe–Fe exchange interactions. Besides the potential economical impact, these materials have been extensively studied for the elucidation of the fundamental aspects of magnetism and the understanding of their transport properties on the basis of their electronic structure [1,3].

In the tetragonal body-centered $ThMn_{12}$-type structure, space-group *I*4/*mmm*, the A atom is located on the origin of the unit cell, equiposition 2*a*, and the other atoms occupy the 8*f*, 8*j* and 8*i* sites (Fig. 1). It is now clear from the refinement of X-ray and neutron diffraction data [4–8] that in these compounds Fe and Al have a strong preference for the 8*f* and 8*i* sites, respectively, and that the 8*j* sites are shared by the remaining Fe and Al.

The study of ideally ordered AFe_4Al_8 stoichiometric compounds, where the sublattices of Fe (magnetic) and Al (non-magnetic) are clearly separated, is a convenient first approach to the understanding of the coupling between the

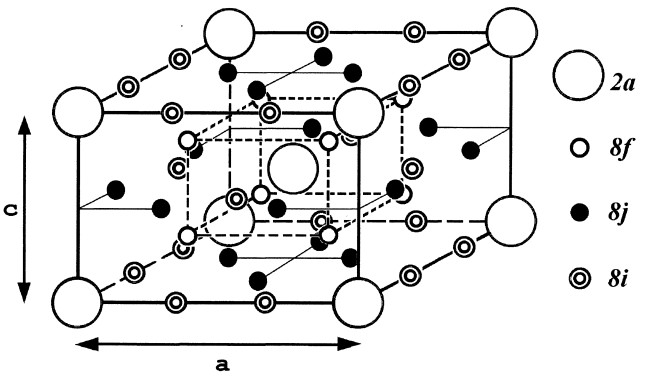

Fig. 1. Crystallographic unit-cell of the $ThMn_{12}$-type structure. The *f*-element atoms are located at the origin and body-centered positions (2*a* sites). The other atoms occupy the 8*f*, 8*j* and 8*i* sites.

*Corresponding author. Tel.: +351-21-994-6220; fax: +351-21-994-1455.

E-mail address: jcarlos@itn1.itn.pt (J.C. Waerenborgh).

0925-8388/01/$ – see front matter
PII: S0925-8388(00)01355-4

magnetic (f and d) sublattices. The particular cases of YFe_4Al_8 and $LuFe_4Al_8$ may give information on the interplay of the Fe atoms when there is no ordered moment on the A atom. The Lu and Y compounds have therefore been the subject of several studies. Published results suggested rather complex magnetic properties but were not always consistent. Early ^{57}Fe Mössbauer data [9,10] indicated that well below the magnetic ordering temperature, $T_{ord} \approx 185$ K, the spectra consisted of a single magnetic splitting. However no details of the temperature dependence of the Fe magnetic hyperfine fields, B_{hf}, were given. Distinct spectra were later reported for YFe_4Al_8 at ≈ 5 K but the main differences should be attributed to the presence of Fe–Al binary alloys [7]. Recent studies made by powder neutron diffraction and ^{57}Fe-Mössbauer spectroscopy have confirmed $T_{ord} \approx 185$ K and have shown that the Fe magnetic moments, μ_{Fe}, give rise to a complex antiferromagnetic (AF) ordering [11].

Recent neutron scattering studies performed on large single crystals grown from melts with YFe_4Al_8 and $LuFe_4Al_8$ composition revealed large discrepancies between the magnetic properties and the magnetic structure of these single crystals and those reported for the same samples prepared as a polycrystalline material [12]. In contrast to UFe_4Al_8 [13] the Y single crystals have final composition $YFe_{4.2}Al_{7.8}$ [7]. Differences of 1–2% in the site occupation factors are difficult to detect from the refinement of X-ray diffracted intensities. However the magnetic interactions in these compounds are extremely sensitive to their exact composition. Besides a drop in T_{ord} from ≈ 180 K down to ≈ 100 K strikingly different ^{57}Fe Mössbauer spectra are obtained for AFe_4Al_8 and AFe_xAl_{12-x} (A=U and Y, $4 < x < 4.3$), due to the strong dependence of B_{hf} on the number of Fe nearest neighbours, NN [7,14]. Recent refinements of the Bragg intensities obtained from single-crystal neutron diffraction data have confirmed that the composition of the Y and Lu single crystals is AFe_xAl_{12-x} with $4.2 \leq x \leq 4.4$ [15].

A detailed investigation of the relation between magnetic and structural properties of the A–Fe–Al ternary systems was undertaken by us in the last years. In this paper, the present status of the ^{57}Fe-Mössbauer study of the AFe_xAl_{12-x} compounds $4 \leq x \leq 4.3$ is reviewed. New data on UFe_4Al_8 prepared as single-crystalline material, $LuFe_{4.1}Al_{7.9}$ and $TmFe_4Al_8$ are also presented. Excluding the cases of non-magnetic A, $TmFe_4Al_8$ is the AFe_4Al_8 intermetallic where the A sublattice is reported to order at the lowest temperature, below 4.2 K [16].

2. Experimental

The starting materials, Fe, Al and A=Y, Tm, Lu and U metals, for the preparation of the ternary alloys were used in the form of ingots with purity higher than 99.9%. Bulk charges with nominal AFe_4Al_8 compositions were prepared. All of them were arc melted under high-purity argon on a water-cooled copper crucible. To ensure homogeneity the obtained buttons were turned around and melted at least twice. The weight losses during melting were less than 1%. Samples prepared as polycrystalline material were annealed under vacuum at 1070 K for 30 days.

Large single crystals were grown from AFe_4Al_8 (A=Y, Lu and U) bulk charges, in an induction furnace with a levitation cold crucible, by the Czochralski method, using a tungsten needle as a seed. A pulling rate of 2 cm/h and a rotation rate of 15 rpm were employed. Part of these pulled materials were ground and studied as powder samples.

Finely ground powder of each sample prepared was back pressed into standard aluminum holders for powder X-ray diffraction (XRD). Diffracted X-ray intensities were collected on a Philips automated diffractometer system PW1710. A PW1820 Bragg Brentano goniometer fitted with a PW1752 curved graphite crystal monochromator, incident and diffracted beam Soller slits, one divergence and antiscatter slits and a 0.2 mm receiving slit, was used. The intensity measurements were made with a normal focus Cu tube operated at 40 kV and 30 mA and using a take-off angle of 5°. The data were recorded with a 2θ-step size of 0.02° in a 2θ-range of 18.00–100.00° and a counting time of 13 s at each step.

All the diffraction peaks which did not correspond to a $ThMn_{12}$-type phase could be assigned to the strongest peaks of the A–Al or the Fe–Al binary alloys referred below, by comparing the experimental data with either the PDF-data base [17] or, in the case of Lu–Al alloys with simulated powder diffractograms [18] based on published crystallographic data [19]. In order to confirm the presence of these additional phases it was checked if all the strongest peaks of the identified binary alloys were either present or overlapping the peaks of the $ThMn_{12}$-type phase. The least-squares structure refinements of the $ThMn_{12}$-type phases were undertaken with the Rietveld powder profile program [18] assuming space-group $I4/mmm$. Details of these refinements are described elsewhere [7].

Magnetization measurements were performed on powder samples using a SQUID magnetometer (MPMS Quantum Design). The magnetization was measured as a function of temperature in the range 5–300 K, under low applied fields (≤ 50 mT) after both zero-field-cooling (ZFC) and field-cooling (FC) procedures (M vs. T curves). Magnetization was also obtained as a function of applied field for fields up to 5.5 T and for different constant temperature values (M vs. B curves).

Powdered samples were pressed together with lucite powder into perspex holders, in order to obtain homogeneous and isotropic Mössbauer absorbers containing ~5 mg/cm^2 of natural iron. The ^{57}Fe Mössbauer-spectroscopy results were obtained in the transmission mode using a constant-acceleration spectrometer and a 25 mCi ^{57}Co

source in Rh matrix. The velocity scale was calibrated using an α-Fe foil at room temperature. Spectra were collected at several temperatures between 300 and 5 K. Low-temperature spectra were obtained using a flow cryostat with temperature stability of ±0.5 K. The spectra were fitted to Lorentzian lines. The fitting procedure was the same used in the case of the UFe_xAl_{12-x} intermetallics and is described in detail elsewhere [14].

3. Results

3.1. $TmFe_4Al_8$

The powder XRD data of the $TmFe_4Al_8$ sample annealed at 1070 K show no traces of impurity phases. The Rietveld analysis of the diffracted intensities is consistent with the nominal composition of the compound and indicates that Fe is only present on the 8*f* site (Table 1).

As in the case of YFe_4Al_8 prepared as a polycrystalline sample and annealed at 1070 K [7], the room temperature Mössbauer spectrum consists of a symmetric doublet: linewidths and relative areas of each peak are equal within experimental error. Furthermore the Mössbauer spectrum taken at 5 K (Fig. 2) shows a single sextet with an estimated B_{hf} of 10.7 T (Table 2) in agreement with published results [10]. These results are consistent with each kind of atom being present on only one crystallographic site clearly confirming the XRD data.

As the temperature increases, although only six lines are observed (Fig. 2), the widths and the relative intensities of these lines deviate more and more from the theoretical expected values. If more than on sextet is considered, the

Table 1
Crystallographic data including estimated atomic positions (*x*, *y*, *z*), site occupations (in atoms/f.u.) and equivalent isotropic temperature factors (B_{eq}) from the Rietveld analysis of the powder XRD data

Sample	$LuFe_4Al_8$ 1070 K	$TmFe_4Al_8$ 1070 K
Space group (No. 139)	*I*4/*mmm*	*I*4/*mmm*
Lattice parameters (at 300 K), Å		
a	8.7072(3)	8.716(1)
c	5.0353(3)	5.0367(9)
Cell volume, $Å^3$	381.75(3)	382.6(1)
Radiation	Cu Kα	Cu Kα
2θ range	21–100°	20–100°
Site occupation Y 2*a*	1.00(1)	0.99(5)
Fe 8*f*	4.0(1)	3.9(1)
Al 8*j*	4.0(1)	4.0(1)
Al 8*i*	4.1(1)	4.0(1)
B_{eq} ($Å^2$) Y 2*a*	0.50	0.54
Fe 8*f*	0.50	0.57
Al, Fe 8*j*	0.49	0.44
Al 8*i*	1.01	0.44
Site 8*j* (x_1, 1/2, 0)	0.2719(5)	0.2797(8)
Site 8*i* (x_2, 0, 0)	0.3446(7)	0.343(1)
Agreement factors		
R_{Bragg}, R_F (%)	9.70, 6.70	4.06, 3.11
Formula obtained from site occupations	$LuFe_{4.0(2)}Al_{8.1(2)}$	$TmFe_{4.0(2)}Al_{8.0(2)}$

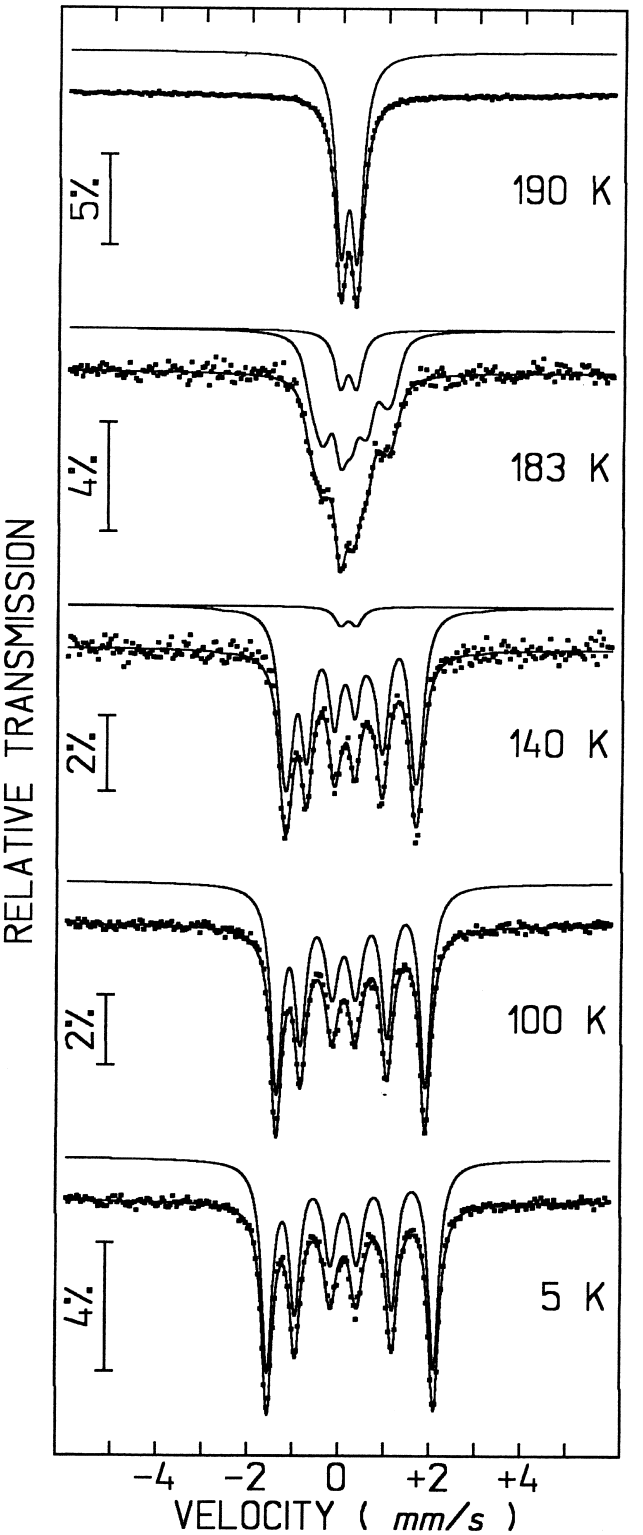

Fig. 2. ^{57}Fe Mössbauer spectra taken at different temperatures of the $TmFe_4Al_8$ sample prepared as polycrystalline material and annealed at 1070 K.

Table 2
Estimated parameters from the Mössbauer spectra of samples prepared as polycrystalline material (p) or as large single crystals (sc)[a]

T	Sample	Site	z	I (%)	δ (mm/s)	Δ, ε (mm/s)	Γ (mm/s)	B_{hf} (T)
295 K	YFe_4Al_8 (p)	8*f*	2	100	0.18	0.31	0.30	–
295 K	$TmFe_4Al_8$ (p)	8*f*	2	100	0.18	0.34	0.30	–
295 K	UFe_4Al_8 (sc)	8*f*	2	100	0.16	0.30	0.30	–
5 K	YFe_4Al_8 (p)	8*f*	2	100	0.31	0.14	0.38	10.7
5 K	$YFe_{4.2}Al_{7.8}$ (sc)	8*j*	≥4	4.8	0.18	0.47	0.27	18.6
		8*f*	≥3	17.7	0.26	0.18	0.25	13.9
		8*f*	2	77.5	0.31	0.14	0.30	10.7
5 K	$TmFe_4Al_8$ (p)	8*f*	2	100	0.31	0.15	0.34	11.3
5 K	UFe_4Al_8 (sc)	8*f*	2	100	0.28	0.13	0.32	11.0
5 K	$LuFe_{4.1}Al_{7.9}$ (p)	8*j*	≥4	2.5	0.23	0.59	0.35	19.3
		8*f*	≥3	9.0	0.25	0.24	0.36	14.1
		8*f*	2	88.5	0.31	0.14	0.38	10.9

[a] I, relative areas, are fixed, consistent with the calculated probabilities for the different number of Fe NN (z) of Fe atoms on the 8*f* and 8*j* sites. δ, isomer shift relative to metallic α-Fe at 295 K; Δ, quadrupole splitting (at 295 K); $\varepsilon=(e^2 V_{zz}Q/4)(3\cos^2\theta-1)$, quadrupole shift (at 5 K). Γ, line-widths of the two inner peaks of a sextet; B_{hf}, magnetic hyperfine field. Estimated errors for δ, Δ, and Γ of doublets with $I>15\%$ are ≤0.02 mm/s and of the others ≤0.04 mm/s. Estimated errors for the sextets with $I>11\%$ are ≤0.2 T for B_{hf}, ≤0.02 mm/s for δ, ε, Γ, and for the others ≤0.4 T for B_{hf}, ≤0.03 mm/s for δ, and ≤0.04 mm/s for Γ and ε.

ratio of the relative areas $I_{1,6}/I_{2,5}/I_{3,4}$ may be kept equal to 3:2:1 for each sextet and the linewidths of each line pair increase only slightly from the inner to the outer lines. The spectrum at 100 K (Fig. 2) was fitted by a narrow distribution of B_{hf} with the same isomer shift and quadrupole shift. Between 140 and 183 K, besides this distribution, which has a much larger width than at 100 K, the fit is considerably improved if a paramagnetic doublet is considered. The relative intensity of this doublet increases with temperature. Finally at 190 K all the Fe is paramagnetic (Fig. 2).

The main difference between the M vs. T curves of $TmFe_4Al_8$ and YFe_4Al_8 [7] is the strong increase of the magnetization of $TmFe_4Al_8$ below ≈20 K (Fig. 3a). This increase may be explained by the ferromagnetic ordering of the Tm sublattice occurring below 4.2 K [16]. No maximum is observed in the M vs. T curves down to 2 K, even in a field of 5 mT. However, M vs. B curves above 10 K show an antiferromagnetic-like behaviour due to the ordering of the Fe sublattice while at 2 K they show a ferromagnetic-like behaviour, certainly due to the ordering of the Tm sublattice (Fig. 3b).

Features of the M vs. T curves of $TmFe_4Al_8$ above the ordering temperature of Tm may be correlated with the Mössbauer results as in the case of YFe_4Al_8[7]. The Y compound also shows a temperature range where paramagnetic and magnetically ordered Fe coexist. The highest temperature at which magnetically ordered Fe is observed in the Mössbauer spectra corresponds to a broad maximum of both the FC and ZFC curves at ≈180 K. Finally, a second maximum in the ZFC and a change in slope in the FC curve are observed around 130 K. Although there is no sharp transition in the shapes of the Mössbauer spectra taken above and below this temperature it is noteworthy that 140 K is the lowest temperature at which there is an improvement in the fit of the Mössbauer spectrum if a quadrupole splitting is considered, strongly suggesting that it is only below 140 K that all the Fe atoms are magnetically ordered.

3.2. UFe_4Al_8 prepared as a single crystal

In agreement with previous results [13,20] Mössbauer spectra, taken at 5 K and above 155 K, of the UFe_4Al_8 material prepared as single crystals (Fig. 4) show that the Fe atoms fully occupy the 8*f* sites and that above 150 K all the Fe atoms are paramagnetic. At intermediate temperatures however a situation similar to that observed for $TmFe_4Al_8$, YFe_4Al_8 [7] and UFe_4Al_8 prepared as polycrystalline material [21] occurs. A distribution of B_{hf} is observed within the range ≈100–150 K and between ≈140 and 150 K paramagnetic Fe coexist with magnetically ordered Fe. However no singularities in the M vs. T curves of UFe_4Al_8 [20] similar to those of YFe_4Al_8 and $TmFe_4Al_8$ are observed. This is probably due to the ferromagnetic ordering of the U sublattice [13,20]. The dominant effect of the U magnetization on the global M vs. T curve may conceal the smaller oscillations due to the temperature dependent rearrangements of the Fe magnetic sublattice.

3.3. AFe_4Al_8 (A=Y and Lu, 4≤x≤4.3)

The Mössbauer spectra taken at room temperature of samples obtained from powdering material pulled from melted bulk charges containing A (A=Lu,Y), Fe and Al in the atomic ratios 1/4/8, always show an asymmetric doublet, in contrast to the spectra of UFe_4Al_8 obtained in the same way and those of AFe_4Al_8 (A=Y, Tm, U) prepared as polycrystalline materials and annealed at 1070 K [7]. The spectra taken at 5 K (Fig. 5) are similar to those obtained for $UFe_{4.2}Al_{7.8}$ and $YFe_{4.2(2)}Al_{7.8(2)}$ [7,14]. They may be fitted by three magnetic splittings whose hyperfine parameters and relative intensities may be understood in

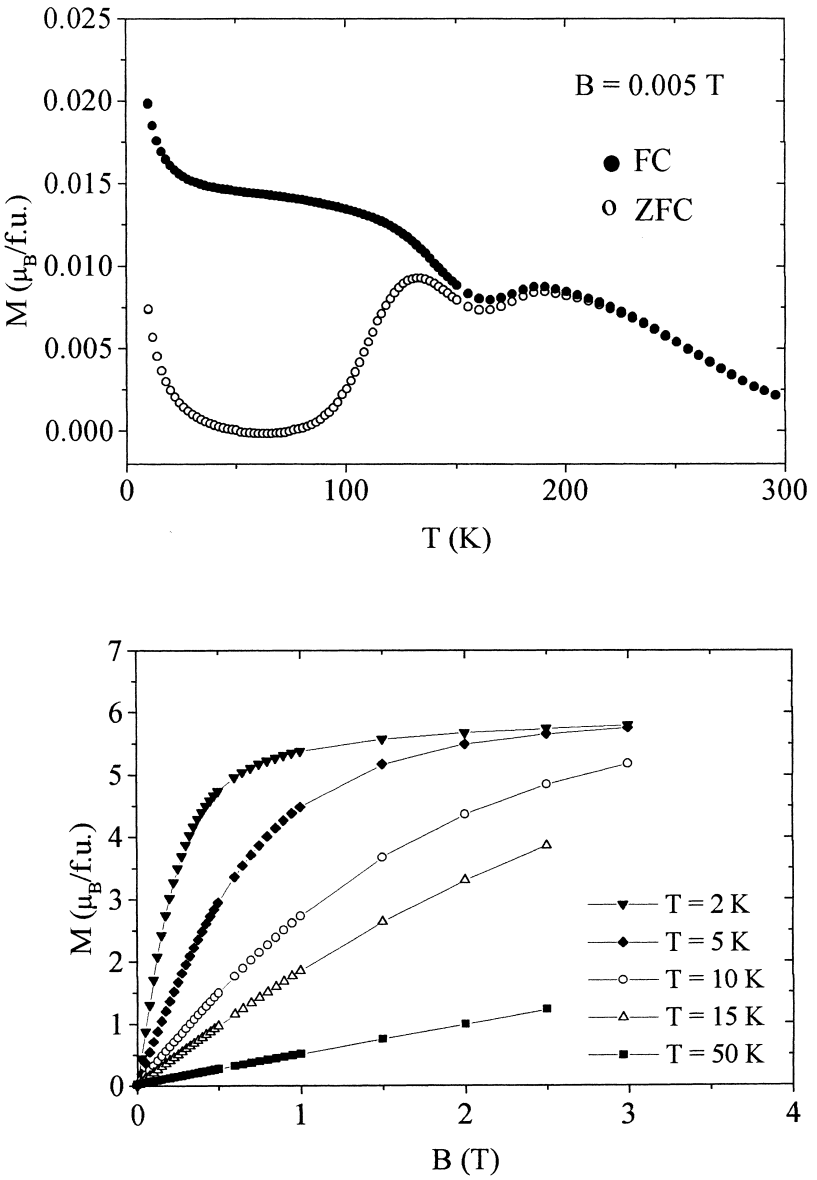

Fig. 3. Magnetization (M) vs. temperature in a field B = 0.005 T (a), and vs. external field at different temperatures (b), of the $TmFe_4Al_8$ sample prepared as polycrystalline material and annealed at 1070 K.

the light of proper physical models [14], assuming compositions $YFe_{4.2}Al_{7.8}$ or $LuFe_{4.3}Al_{7.7}$ [7,15] and that Fe fully occupies the 8*f* sites and share the 8*j* sites with Al. In AFe_xAl_{12-x} ($4 \leq x \leq 4.3$) the Fe atoms on the 8*f* sites have two Fe NN on other 8*f* sites. In AFe_xAl_{12-x} ($x = 4.2$, 4.3) some of them may also have a third Fe NN located on a 8*j* site. The relative intensities, *I*, of the magnetic splittings arising from Fe atoms with different configurations may be calculated assuming a random occupation of the 8*j* sites by Fe and Al (Table 2). The probabilities of the configurations with more than 3 Fe NN for Fe atoms on the 8*f* sites and more than 4 Fe NN for Fe atoms on the 8*j* sites correspond to magnetic sextets with $I < 1.5\%$.

In contrast to YFe_4Al_8 and $TmFe_4Al_8$ prepared as a polycrystalline material and annealed at 1070 K, the powder XRD data of the sample containing Lu, Fe and Al in the atomic ratios 1/4/8 and obtained through the same procedure, still show the strongest diffraction peaks of Fe_3Al_{14}, Fe_2Al_5, $LuAl_3$ and $LuAl_2$. The refinement of the main $ThMn_{12}$-type phase was however performed. The estimated site occupation factors give no evidence of the presence of Fe on the 8*j* site and are consistent with $LuFe_{4.0(2)}Al_{8.1(2)}$ composition (Table 1). However, the 5 K Mössbauer spectrum clearly denotes the presence of Fe atoms on the 8*j* site (Fig. 6). Small shoulders are apparent on the outer peaks of the low-temperature sextet. Carrying out the analysis of the spectrum based on the above referred model the best fit is obtained assuming composition $LuFe_{4.1}Al_{7.9}$ (Table 2). This composition is consistent with the values estimated for the site occupation

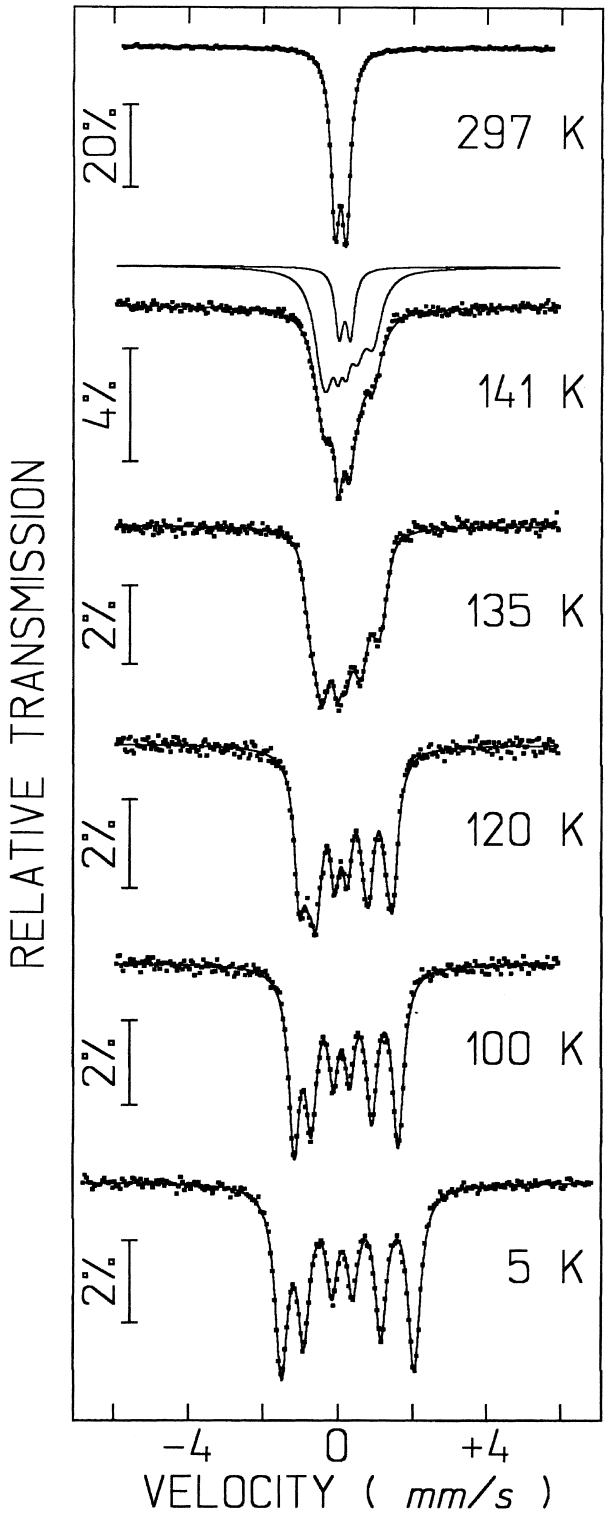

Fig. 4. ^{57}Fe Mössbauer spectra taken at different temperatures of a powdered UFe_4Al_8 sample prepared as a large single crystal by the Czochralski method.

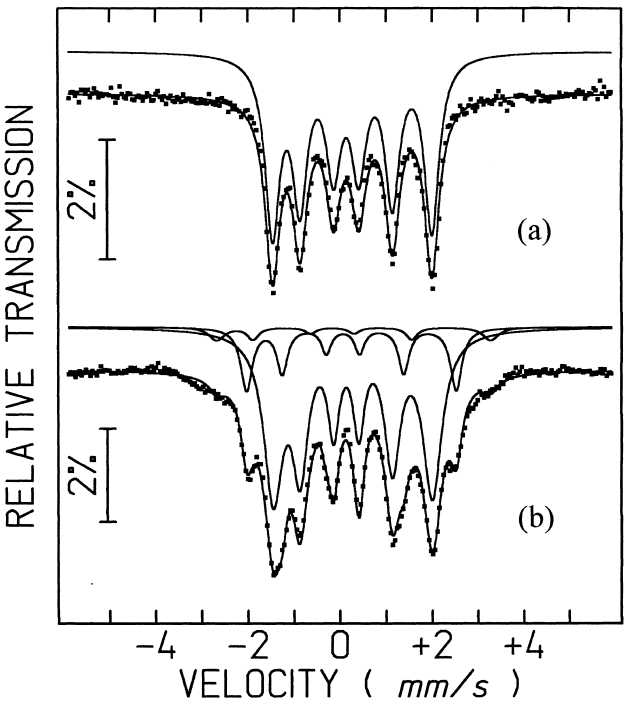

Fig. 5. Comparison between the ^{57}Fe Mössbauer spectra taken at 5 K of (a) the YFe_4Al_8 sample prepared as polycrystalline material and annealed at 1070 K, and (b) the powdered single crystal grown from a bulk charge containing Y, Fe and Al in the atomic ratios 1/4/8 but with the actual composition $YFe_{4.2}Al_{7.8}$.

factors from the XRD data refinement, considering the calculated uncertainties (Table 1). Mössbauer data are more sensitive to the presence of 8*j* Fe atoms than the site occupation factors estimated from powder XRD, due to the large effect of the 8*j* Fe atoms on the B_{hf} of the 8*f* Fe NN atoms.

Between 60 and 180 K, the Mössbauer spectra of $LuFe_{4.1}Al_{7.9}$ can only be fitted by a continuous distribution of B_{hf} as observed in the case of $LuFe_{4.3}Al_{7.7}$ [15] and of the above referred AFe_4Al_8 intermetallics. The exact magnetic behaviour of the Fe sublattices in each of the Lu compounds is, however, different. In $LuFe_{4.3}Al_{7.7}$ between 100 and 105 K all the Fe atoms become paramagnetic. Furthermore, if a quadrupole doublet is considered, the refinement of the Mössbauer spectra of $LuFe_{4.1}Al_{7.9}$ is significantly improved even for temperatures as low as 69 K. The relative intensity of this quadrupole doublet increases with temperature but the B_{hf} distribution is still observed up to 180 K (Fig. 6). This suggests that although the magnetic ordering of the Fe atoms starts between 180 and 190 K in $LuFe_{4.1}Al_{7.9}$, paramagnetic Fe is still present at 60 K. The 180–190 K temperature range is in agreement with T_{ord} reported for $LuFe_4Al_8$ prepared as polycrystalline material [10,11]. The reported B_{hf} of 10.8 T for $LuFe_4Al_8$ [10] is equal to the B_{hf} estimated in Table 2 for the Fe atoms on the 8*f* sites with 2 Fe NN in $LuFe_{4.1}Al_{7.9}$, and slightly larger than the corresponding one in $LuFe_{4.3}Al_{7.7}$ [15]. In YFe_xAl_{12-x} [7] an almost constant value of this B_{hf} was also observed within the range $4 \leq x \leq 4.2$, while for UFe_xAl_{12-x} a decrease as x increases was detected [14]. The deviation of the composition of our sample from the ideal $LuFe_4Al_8$ may be justified by the

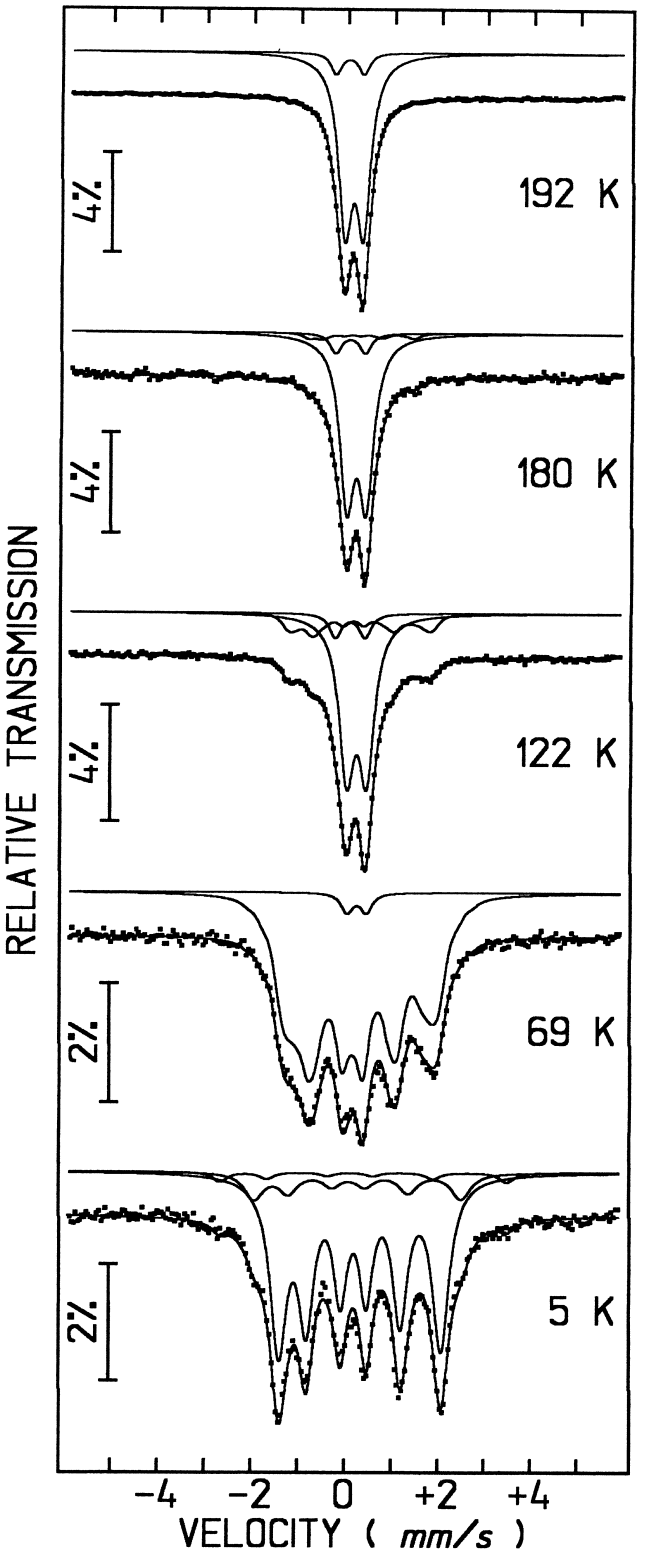

Fig. 6. ^{57}Fe Mössbauer spectra taken at different temperatures of a $LuFe_{4.1}Al_{7.9}$ sample obtained from a bulk charge containing Lu, Fe and Al in the atomic ratios 1/4/8 and annealed at 1070 K.

presence of Fe–Al and Lu–Al binary alloys. Different annealing temperatures will be tried hoping to stabilize the $LuFe_4Al_8$ phase.

4. Conclusion

The same model that explains the ^{57}Fe-Mössbauer spectra of intermetallics of the UFe_xAl_{12-x} series [14] where the A sublattice orders magnetically at the same temperature as the Fe sublattice [13,20], is also successfully used for the Y and Lu analogs where the A element is non-magnetic. Although the magnetic interactions of the A element are quite diverse in these compounds, the temperature dependence of the distribution of the B_{hf} seems to be much the same. As similar trends are expected for B_{hf} and μ_{Fe}, this strongly suggests that μ_{Fe} are also very sensitive to the number of Fe NN.

This property allows a clear distinction between the ^{57}Fe-Mössbauer spectra of the AFe_4Al_8 and $AFe_{4.2}Al_{7.8}$, which has made evident that the large single crystals grown out of charges with YFe_4Al_8 and $LuFe_4Al_8$ compositions were actually richer in Fe. In the case of UFe_4Al_8, however, both large single-crystals and samples prepared as polycrystalline material have the same final composition.

The high sensitivity of the μ_{Fe} on small deviations of the ideal composition of the AFe_4Al_8 is not only observed when excess Fe atoms are present. The ^{57}Fe-Mössbauer data taken at intermediate temperatures of YFe_4Al_8, $TmFe_4Al_8$ and UFe_4Al_8 can only be explained if not all the Fe atoms have the same μ_{Fe}. Since the presence of Fe atoms on the 8*j* sites are expected to have a completely different effect on the Mössbauer spectra than those shown in Figs. 2 and 4, these anomalies may tentatively be attributed to the presence of vacancies. In fact, considering the estimated uncertainties for the site occupation factors the presence of 0.2 vacancies per formula unit on each site can not be ascertained from the Rietveld analysis alone. Such a concentration of this kind of defects is also too low to produce any asymmetry in either the magnetic or the quadrupole splittings observed in the Mössbauer spectra obtained at 5 K or above 180 K, respectively. However, at intermediate temperatures, between T_{ord} and 50–100 K, μ_{Fe} seem to be highly sensitive to very small alterations on the Fe neighbourhood. Therefore, the exact temperature range and shape of the B_{hf} distribution will probably be dependent on small details of the synthesis procedure.

Care in the preparation and structural characterization of these intermetallics should therefore be emphasized, since small deviations in composition have drastic effects on their magnetic properties explaining most of the contradictory results published in the literature.

Acknowledgements

This work was supported by PRAXIS (Portugal) under contract nr. P/FIS/10040/98. The stay of P.S. in Portugal was supported by a NATO grant.

References

[1] W. Suski, The $ThMn_{12}$-type compounds of rare-earths and actinides: structure, magnetic and related properties, in: K.A. Gschneider Jr., L. Eyring (Eds.), Handbook on the Physics and Chemistry of Rare Earths, Vol. 22, Elsevier, Amsterdam, North Holland, 1996.
[2] C. Piquer, M. Artigas, J. Rubín, J. Bartolomé, J. Phys.: Condens. Matter 10 (1998) 11055.
[3] K.H.J. Buschow, J. Alloys Comp. 193 (1993) 223.
[4] I.J. Felner, J. Less-Comm. Met. 72 (1980) 241.
[5] K.H.J. Buschow, J. Less-Comm. Met. 50 (1976) 145.
[6] O. Moze, R.M. Ibberson, K.H.J. Buschow, J. Phys.: Cond. Matter 2 (1990) 1677.
[7] J.C. Waerenborgh, P. Salamakha, O. Sologub, A.P. Gonçalves, C. Cardoso, S. Sério, M. Godinho, M. Almeida, Chem. Mater. 12 (2000) 1743.
[8] J.A. Paixão, M. Ramos Silva, S.Aa. Sörensen, B. Lebech, G.H. Lander, P.J. Brown, S. Langridge, E. Talik, A.P. Gonçalves, Phys. Rev. B 61 (2000) 6176.
[9] A.M. Van der Kraan, K.H.J. Buschow, Physica B 86–88 (1977) 93.
[10] K.H.J. Buschow, A.M. Van der Kraan, J. Phys. F 8 (1978) 921.
[11] P. Schobinger-Papamantellos, K.H.J. Buschow, C. Ritter, J. Magn. Magn. Mater. 186 (1998) 21.
[12] J.A. Paixão, S. Langridge, S.Aa. Sørensen, B. Lebech, A.P. Gonçalves, G. Lander, P.J. Brown, P. Burlet, E. Talik, Physica B 234 (1997) 614.
[13] J.A. Paixão, B. Lebech, A.P. Gonçalves, P.J. Brown, G.H. Lander, P. Burlet, A. Delapalme, J.C. Spirlet, Phys. Rev. B 55 (1997) 14370.
[14] J.C. Waerenborgh, A.P. Gonçalves, M. Almeida, Solid State Commun. 110 (1999) 369.
[15] J.A. Paixão, M. Ramos Silva, J.C. Waerenborgh, A.P. Gonçalves, G.H. Lander, P.J. Brown, M. Godinho, P. Burlet, Phys. Rev. B (2001) in press.
[16] P.C.M. Gubbens, A.M. Van der Kraan, K.H.J. Buschow, J. Magn. Magn. Mater. 27 (1982) 61.
[17] Selected Powder Diffraction Data for Metals and Alloys, Ed. JCPDS Int. Centre for Diffraction Data: Swarthmore, Pennsylvania 19081, USA, 1978.
[18] J. Rodriguez-Carvajal, Physica B 192 (1993) 55.
[19] P. Villars, L.D. Calvert, Pearson's Handbook of Crystallographic Data for Intermetallic Phases, ASM International, Materials Park, OH, USA, 1991.
[20] M. Godinho, G. Bonfait, A.P. Gonçalves, M. Almeida, J.C. Spirlet, J. Magn. Magn. Mater. 140–144 (1995) 1417.
[21] J. Gal, I. Yaar, D. Regev, S. Fredo, G. Shani, E. Arbaboff, W. Potzel, K. Aggarwal, J.A. Pereda, G.M. Kalvius, F.J. Litterst, W. Schafer, G. Will, Phys. Rev. B 42 (1990) 8507.